Whole-genome sequencing identifies a recurrent functional synonymous mutation in melanoma

Jared J. Gartner[a,1], Stephen C. J. Parker[a,1], Todd D. Prickett[a], Ken Dutton-Regester[b], Michael L. Stitzel[a], Jimmy C. Lin[c], Sean Davis[d], Vijaya L. Simhadri[e], Sujata Jha[f], Nobuko Katagiri[e], Valer Gotea[a], Jamie K. Teer[a], Xiaomu Wei[a], Mario A. Morken[a], Umesh K. Bhanot[g], NISC Comparative Sequencing Program[a,2], Guo Chen[h], Laura L. Elnitski[a], Michael A. Davies[h], Jeffrey E. Gershenwald[h], Hannah Carter[i], Rachel Karchin[i], William Robinson[j], Steven Robinson[j], Steven A. Rosenberg[d], Francis S. Collins[a], Giovanni Parmigiani[k,l], Anton A. Komar[f], Chava Kimchi-Sarfaty[e], Nicholas K. Hayward[b], Elliott H. Margulies[a,m], and Yardena Samuels[a,n,3]

[a]National Human Genome Research Institute and [d]National Cancer Institute, National Institutes of Health, Bethesda, MD 20892; [b]Division of Genetics and Computational Biology, Queensland Institute of Medical Research, Brisbane, QLD 4006, Australia; [c]Department of Pathology and Immunology, Washington University School of Medicine, St. Louis, MO 63110; [e]Laboratory of Hemostasis, Division of Hematology, Center for Biologics Evaluation and Research, Food and Drug Administration, Bethesda, MD 20892; [f]Center for Gene Regulation in Health and Disease and the Department of Biological, Geological, and Environmental Sciences, Cleveland State University, Cleveland, OH 44115; [g]Department of Pathology, Memorial Sloan-Kettering Cancer Center, New York, NY 10065; [h]Department of Melanoma Medical Oncology, University of Texas MD Anderson Cancer Center, Houston, TX 77030; [i]Department of Biomedical Engineering, Institute for Computational Medicine, Johns Hopkins University, Baltimore, MD 21218; [j]Division of Medical Oncology, University of Colorado School of Medicine, Aurora, CO 80045; [k]Department of Biostatistics and Computational Biology, Dana Farber Cancer Institute, Boston, MA 02115; [l]Department of Biostatistics, Harvard School of Public Health, Boston, MA 02115; [m]Illumina United Kingdom, Chesterford Research Park, Little Chesterford, Nr Saffron Walden, Essex CB10 1XL, United Kingdom; and [n]Department of Molecular Cell Biology, Weizmann Institute of Science, Rehovot 76100, Israel

Edited* by Bert Vogelstein, Johns Hopkins University, Baltimore, MD, and approved June 27, 2013 (received for review March 12, 2013)

Synonymous mutations, which do not alter the protein sequence, have been shown to affect protein function [Sauna ZE, Kimchi-Sarfaty C (2011) *Nat Rev Genet* 12(10):683–691]. However, synonymous mutations are rarely investigated in the cancer genomics field. We used whole-genome and -exome sequencing to identify somatic mutations in 29 melanoma samples. Validation of one synonymous somatic mutation in *BCL2L12* in 285 samples identified 12 cases that harbored the recurrent F17F mutation. This mutation led to increased *BCL2L12* mRNA and protein levels because of differential targeting of WT and mutant *BCL2L12* by hsa-miR-671–5p. Protein made from mutant *BCL2L12* transcript bound p53, inhibited UV-induced apoptosis more efficiently than WT *BCL2L12*, and reduced endogenous p53 target gene transcription. This report shows selection of a recurrent somatic synonymous mutation in cancer. Our data indicate that silent alterations have a role to play in human cancer, emphasizing the importance of their investigation in future cancer genome studies.

Systematic melanoma whole-exome and -genome studies have uncovered numerous recurrent mutations as well as highly mutated genes that show functional consequences on melanoma growth (1–6). These studies focus exclusively on coding mutations and specifically on nonsynonymous mutations, insertion/deletion mutations as well as splice sites. Recently, noncoding mutations in the telomerase reverse transcriptase (*TERT*) promoter have been shown to generate new E-twenty-six (ETS) transcription factors binding motifs, leading to increased expression of telomerase reverse transcriptase (7, 8). These studies highlight the importance of adjusting our focus beyond the nonsynonymous coding mutations and evaluating all mutations in melanoma.

To gain additional insight into the molecular alterations of melanoma, we report the sequence analysis of 29 melanoma samples and corresponding normal DNA. We performed whole-genome sequencing on 10 matched normal and metastatic tumor DNAs and reanalyzed a previously published melanoma whole-genome study (9, 10). Together with our previous whole-exome analysis of 14 melanoma samples (1) and an additional whole-exome analysis of four matched melanoma and normal samples, this study allows for an unbiased search for unique melanoma genes in a total of 29 samples from treatment naïve patients.

Results

In combined analysis, 13,098 somatic mutations were identified in gene coding regions. Of these mutations, 8,619 caused protein changes, including 7,974 missense, 514 nonsense, 27 small deletion, 11 insertion, and 93 splice site mutations. There were 4,479 silent (synonymous) substitutions (Dataset S1). A nonsynonymous to synonymous ratio of 1.93:1 was calculated, which is not higher than the nonsynonymous to synonymous ratio of 2.5:1 predicted for nonselected mutations (11), suggesting that most are likely passenger mutations. The number of C > T/G > A transitions was significantly greater than other nucleotide substitutions ($P < 0.001$) (*SI Appendix*, Fig. S1), which is consistent with a UV radiation (UVR) signature (12).

Recurrent nonsynonymous mutations, including v-raf murine sarcoma viral oncogene homolog B1 (BRAF) V600E and transformation/transcription domain-associated protein (TRRAP) S722F substitutions, were found (1, 13) as well as 16 recurrent synonymous mutations (Table 1). Although synonymous mutations do not alter the protein sequence, they have been shown to affect protein levels and function (14, 15). However, to date, synonymous mutations have not been investigated in numerous published cancer genomes. We sought to determine whether these somatic synonymous mutations have a functional role in melanomagenesis. Additional screening of these 16 synonymous hotspot mutations in an additional 169 melanoma samples identified olfactory receptor family 4 subfamily C, member 3 (*OR4C3*) and *BCL2L12* (*SI Appendix*, Fig. S2) each to have identical synonymous mutations in three and four additional cases, respectively. The frequency of these recurrent alterations in the validation sample is significantly elevated ($P < 1 \times 10^{-7}$ and $P < 1 \times 10^{-11}$), suggesting that they have either undergone

Author contributions: J.J.G., S.C.J.P., T.D.P., and Y.S. designed research; J.J.G., S.C.J.P., T.D.P., K.D.-R., M.L.S., J.C.L., V.L.S., S.J., N.K., V.G., J.K.T., X.W., M.A.M., U.K.B., N.I.S.C.C.S.P., G.C., and L.L.E. performed research; K.D.-R., M.L.S., J.C.L., N.I.S.C.C.S.P., M.A.D., J.E.G., H.C., R.K., W.R., S.R., and S.A.R. contributed new reagents/analytic tools; J.J.G., S.C.J.P., T.D.P., K.D.-R., M.L.S., J.C.L., S.D., V.L.S., S.J., N.K., V.G., J.K.T., X.W., M.A.M., U.K.B., N.I.S.C.C.S.P., G.C., L.L.E., M.A.D., J.E.G., H.C., R.K., W.R., S.R., S.A.R., F.S.C., G.P., A.A.K., C.K.-S., N.K.H., E.H.M., and Y.S. analyzed data; and J.J.G., S.C.J.P., T.D.P., K.D.-R., M.L.S., J.C.L., S.D., V.L.S., S.J., N.K., V.G., J.K.T., X.W., M.A.M., U.K.B., N.I.S.C.C.S.P., G.C., L.L.E., M.A.D., J.E.G., H.C., R.K., W.R., S.R., S.A.R., F.S.C., G.P., A.A.K., C.K.-S., N.K.H., E.H.M., and Y.S. wrote the paper.

The authors declare no conflict of interest.

*This Direct Submission article had a prearranged editor.

Data deposition: The sequence reported in this paper has been deposited in the dbSNP, ClinVar database (accession no. 1057273).

[1]J.J.G. and S.C.J.P. contributed equally to this work.

[2]A complete list of the NISC Comparative Sequencing Program can be found in *SI Text*.

[3]To whom correspondence should be addressed. E-mail: yardena.samuels@weizmann.ac.il.

This article contains supporting information online at www.pnas.org/lookup/suppl/doi:10.1073/pnas.1304227110/-/DCSupplemental.

GENETICS

Table 1. Recurrent synonymous mutations in analysis of 29 melanoma tumors

Gene name	Ref_seq ID	Nucleotide change	Amino acid change	Tumor name
FCRL1	NM_052938.4	C741T	I247I	96T
				91T
OR2T6	NM_001005471.1	C339T	F113F	7T
				32T
PNLIPRP1	NM_006229.2	C600T	F200F	32T
				55T
OR4C3	NM_001004702.1	C114T	F38F	17T
				108T
OR8J3	NM_001004064.1	C186T	F62F	55T
				01T
CPT1A	NM_001876.3	C1638T	F546F	05T
				43T
DNAH9	NM_001372.3	C6333T	F2111F	24T
				01T
BCL2L12	NM_138639.1	C51T	F17F	55T
				81T
PNKP	NM_007254.3	C75T	P25P	32T
				56T
TTN	NM_133378.4	C10167T	F3389F	130T
				23T
POTED	NM_174981.3	G864A	V288V	12T
				26T
GTSE1	NM_016426.6	C1782T	S594S	24T
				55T
OR5H6	NM_001005479.1	C654T	F218F	24T
				Colo-829
FILIP1	NM_015687.2	G2475A	R825R	17T
				24T
PPP1R3A	NM_002711.3	G2844A	T948T	Colo-829
				51T
COL14A1	NM_021110.1	G4050A	R1350R	23T
				32T

Identification of 16 recurrent mutations and their effects on their transcripts. All mutations were validated through Sanger sequencing and subsequently evaluated in additional cohorts of melanoma.

relaxation of purifying selection (16) or been under selection during tumor development. Because *BCL2L12* has previously been linked to tumorigenesis (17), we screened the *BCL2L12* cytosine to thymine change at position 51 (F17F) in another 87 melanoma samples. This screen identified six additional samples with the same alteration. This mutation, thus, occurred in 10 of 256 melanomas ($P < 1 \times 10^{-31}$) in the combined validation study, strongly suggesting that it has a functional role in melanomagenesis. Consistent with this expectation, this nucleotide position displays evidence of selection (*SI Appendix*, Fig. S3), suggesting that sequence variation at this site is not well-tolerated.

Synonymous mutations have been shown to affect gene function by multiple mechanisms, including but not limited to those mechanisms exerting effects on mRNA splicing, protein translation, and expression (18). Our analyses suggest that the synonymous alteration in *BCL2L12* does not affect splicing, because the mutation does not create a guanine thymine (GT) splicing consensus dinucleotide that could compete with the donor splice site of the first exon or encourage the use of seven cryptic GT splice donor sites within its vicinity (*SI Appendix*, Table S1). Next, we determined whether *BCL2L12* allelic expression is affected by the mutation by comparing the levels of mutant and WT *BCL2L12* alleles. We used MALDI-TOF (Sequenom) analysis to quantitatively assess relative allelic abundance in paired cDNA and genomic DNA (gDNA) from melanoma samples and found that, for 9 of 12 samples, the mutant *BCL2L12* T allele was more abundantly expressed than the WT C allele ($P < 0.01$, Wilcoxon rank sum test) (Fig. 1 *A* and *B*). To test if the protein made from mutant *BCL2L12* transcript is expressed more abundantly than WT *BCL2L12*, we constructed WT and mutated versions of *BCL2L12* cDNA and transiently transfected them. We found that the mRNA (*SI Appendix*, Fig. S4) and protein levels (Fig. 1*C*) of mutant *BCL2L12* were significantly increased relative to WT in multiple independent cotransfection experiments using GFP to control for transfection efficiency.

There could be a number of reasons leading to the elevated BCL2L12 protein expression levels: (*i*) increased mRNA levels (noticed above), (*ii*) enhanced mRNA translation, (*iii*) stabilization of protein against degradation, or (*iv*) all of the above. We, however, found no change in elongation/translation rates of the mutant *BCL2L12* mRNA compared with the WT message (*SI Appendix*, Fig. S5) and no change in stability of protein (expressed in vivo and in vitro) to limited proteolysis. These results largely rule out the F17F mutation having effects on BCL2L12 translation and protein stability.

The elevated levels of mutant *BCL2L12* mRNA could be caused by increased transcription or increased RNA stability. The position corresponding to the mutation in *BCL2L12* displays high conservation across the mammalian lineage, suggesting functional constraints other than purely amino acid encoding (*SI Appendix*, Fig. S6*A*). However, position weight matrix scanning and ChIP analyses provide no support for a mechanism involving preferential binding of expressed transcription factors to the WT or mutated *BCL2L12* alleles (*SI Appendix*, Fig. S6 *B–E*). Increased stability of the mutant *BCL2L12* mRNA could be caused by differential binding of protein or microRNA (miRNA) to mutant and WT *BCL2L12* mRNA. Computational analysis showed that several RNA binding proteins may interact with WT and mutant mRNAs in the region close to the site of mutation. However, gel-shift experiments of top candidate proteins did not

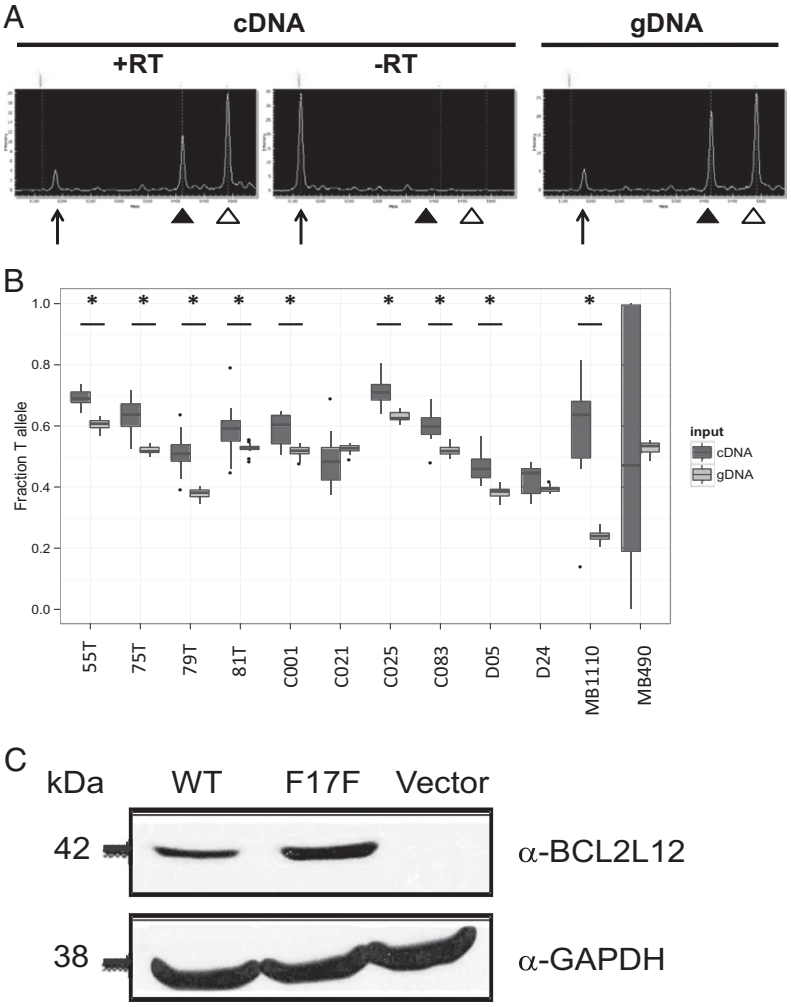

Fig. 1. Abundance of the *BCL2L12* transcript and BCL2L12 protein. (*A*) Image of MALDI-TOF (Sequenom) spectrographs indicating peaks for unextended primer (arrows), C allele (filled arrowheads), and T allele (open arrowheads) for sample 55T cDNA. Unextended primer peak in the −RT control confirms that allelic representation differences in cDNA samples are not because of gDNA contamination. Paired gDNA from each sample was used as a control. (*B*) Box plots show significantly higher T-allele representation in cDNA (dark gray) compared with gDNA (light gray) in 9 of 12 melanoma samples. Significance was calculated from 12 measurements of each cDNA and gDNA sample using the Wilcoxon rank sum test; asterisks indicate samples with $P < 0.01$. (*C*) BCL2L12 protein levels in transiently transfected HEK293T cells (Western blot analysis). Cells were transiently transfected with *BCL2L12* WT or mutant cDNA, and Western blotting was done posttransfection.

reveal any differential binding between the two mRNAs (*SI Appendix*, Fig. S7).

Finally, to evaluate if the mutation affects miRNA binding, we used the miRNA target prediction programs PITA (19) and miRanda (20). A single miRNA (miR) common to both programs, hsa-miR-671–5p, was predicted to bind the WT but not mutant *BCL2L12* transcripts. The miRNA target site in its WT form has high complementarity to mature hsa-miR-671–5p. Furthermore, Genome Evolutionary Rate Profiling (GERP) analysis (21), which identifies evolutionarily constrained positions in multiple genome alignments by quantifying substitution deficits across species, indicates that the target region exhibits high sequence conservation (Fig. 2*A*) (22, 23). We hypothesized that loss of this target site in mutant *BCL2L12* may lead to increased *BCL2L12* transcript levels. hsa-miR-671–5p has been shown previously to be expressed in melanoma (24). Before targeting endogenous *BCL2L12* with hsa-miR-671–5p, we used quantitative RT-PCR (qRT-PCR) analysis to detect the presence of transiently transfected miR mimic in melanoma cell lines (Fig. 2*B*). Furthermore, to show specificity of the miR mimic to target WT *BCL2L12*, we cotransfected WT or mutant *BCL2L12* melanoma cell lines with negative control miR or hsa-miR-671–5p mimic in the presence of a specific miR inhibitor (anti–hsa-miR-671–5p). qRT-PCR analysis shows that anti-miR inhibited and reversed the effect on WT *BCL2L12* message by hsa-miR-671–5p. In mutant cell lines, little to no effect was observed (Fig. 2*C*). The suppression of mature hsa-miR-671–5p mimic by cotransfection with anti–hsa-miR-671–5p was determined by qRT-PCR analysis (*SI Appendix*, Fig. S8). Our results indicate that WT *BCL2L12* mRNA is a target for hsa-miR-671–5p regulation, which leads to its steady state reduction. However, the recurrent *BCL2L12* mutation reduces the affinity of hsa-miR-671–5p binding, thus allowing mutant *BCL2L12* mRNA and protein accumulation.

BCL2L12 was previously shown to be amplified in glioblastoma, to bind p53, and to inhibit apoptosis (17). Together with our identification of a *BCL2L12* hotspot mutation that increases *BCL2L12* expression levels, this finding suggests BCL2L12 to be a candidate unique melanoma oncogene. We, therefore, investigated whether the identified *BCL2L12* C51T mutation may affect apoptosis.

As a first step in assessing this possibility, we confirmed that the mutation does not interfere with p53 binding. Efficient complex formation between endogenous p53 and overexpressed protein transcribed from either WT or mutant *BCL2L12* transcript was seen in HEK293 cells (*SI Appendix*, Fig. S9). The observed interaction with p53, together with the enhanced expression of protein made from mutant *BCL2L12* transcript, may repress p53 activity. This repressed activity may lead to an increased ability of melanoma cells to resist p53-dependent induced apoptosis. To directly test this possibility, we assessed the BCL2L12 antiapoptotic activity after genotoxic stress in melanoma cells that harbor either WT or mutant *BCL2L12*. We used shRNA or siRNA to knockdown *BCL2L12* expression in *BCL2L12* WT (12T and SK-Mel-28) or mutant [75T, 79T (specifically siRNA for 55T), and C025] cells (*SI Appendix*, Figs. S10 and S11). In each case, the knockdown had little to no effect on cells harboring WT *BCL2L12* but significantly reduced the viability of cells harboring mutant *BCL2L12* post-UVR exposure

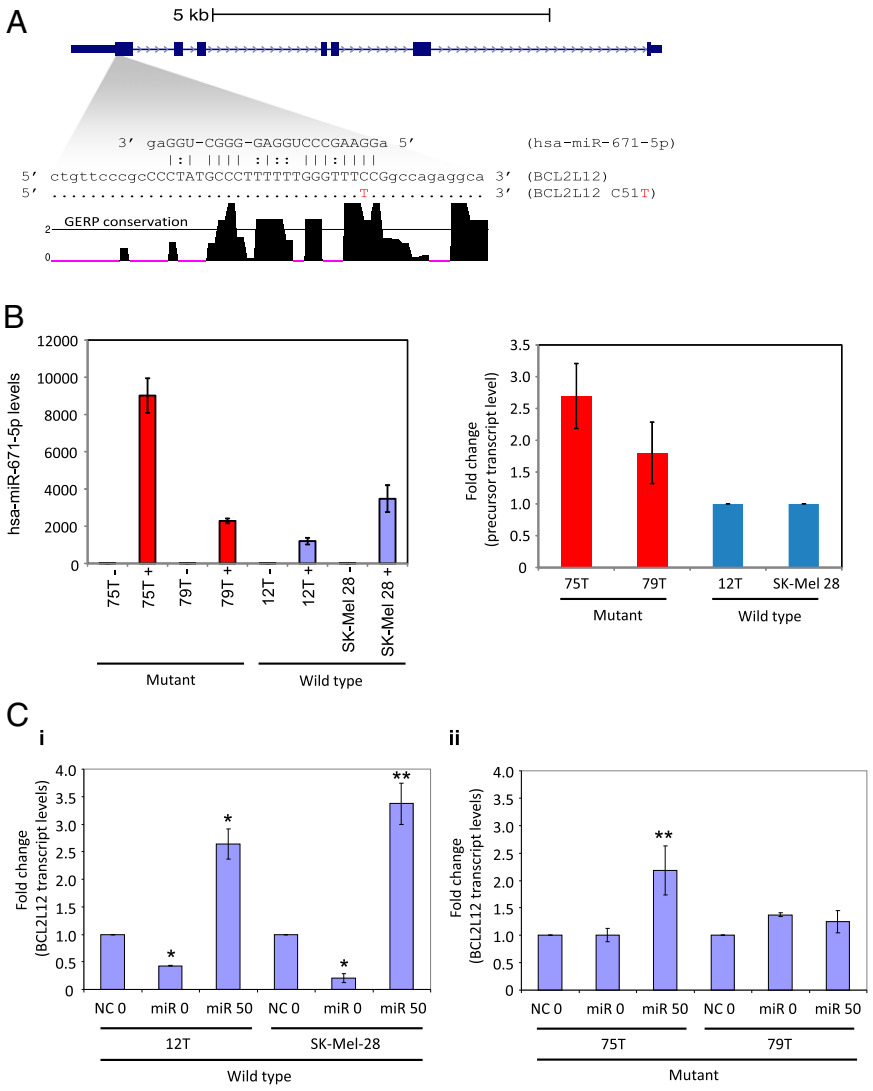

Fig. 2. hsa-miR-671–5p represses WT *BCL2L12* expression. (*A*) Schematic representation of the *BCL2L12* locus at hg18 coordinates chr19:54860211–54868985. Based on miRanda and PITA target scanning predictions, hsa-miR-671–5p binds at the first coding exon and has high affinity to the WT version but not the C51T version. GERP single nucleotide resolution evolutionary conservation scores show that this region is highly conserved. The horizontal line at GERP score = 2 indicates the general threshold that defines evolutionarily constrained bases. For this plot, we only show GERP scores ≥0. (*B*) qRT-PCR analysis of precursor hsa-miR-671 in melanoma cells. Graphs show experimental replicates of qRT-PCR analysis of precursor hsa-miR-671 in mutant *BCL2L12* (75T and 79T) compared with WT *BCL2L12* (12T and SK-Mel-28) cells. Results are representative of two independent experiments. Error bars are SD. (*C*) Anti–miR-671–5p rescues hsa-miR-671–5p–mediated knockdown of WT BCL2L12 in melanoma cells. Graphs show experimental replicates of qRT-PCR of endogenous BCL2L12 levels in (*i*) wild type BCL2L12 (12T and Sk-Mel-28) and (*ii*) mutant BCL2L12 (75T and 79T) cell lines in the presence of negative control miR (NC) or hsa-miR-671–5p (miR) plus 0 or 50 nM anti–miR-671–5p. Results are representative of two independent experiments. Error bars are SD. Comparison of NC0 with miR0 (*$P < 0.01$) or comparison of miR0 with miR50 (**$P < 0.04$; Student *t* test).

(Fig. 3 *A* and *B*). Because BCL2L12 has previously been shown to affect the expression of p53-dependent target genes (17), we tested if depletion of mutant *BCL2L12* in melanoma cells results in differential activation of p53-dependent transcription on UVR treatment compared with *BCL2L12* depletion in WT-expressing cells. Indeed, we observed significant increases in p53-dependent transcription of *MDM2* in mutant cells stably depleted of *BCL2L12* compared with stably depleted WT cells after UVR exposure (Fig. 3*C*). Our results show that synonymous somatic mutations have important roles to play in cancer and also suggest the potential for the prosurvival nature of BCL2L12 in melanoma.

Discussion

We identified a recurrent synonymous somatic mutation in *BCL2L12*. This mutation appears in 12 of 285 samples, suggesting that this mutation is being selected for during tumor development. Analysis of the publicly available TCGA melanoma dataset supports this conclusion, as it also contains this mutation in 8 of 255 samples. Our study shows that the *BCL2L12* synonymous mutation has no effect on normal protein function but instead, causes an accumulation of *BCL2L12* mRNA and protein.

Functional analysis of the mutated form of *BCL2L12* suggests that the mutant's stability leads to overexpression, increasing the antiapoptotic signaling in melanoma cells and promoting cell survival, which may lead to increased resistance to p53-dependent apoptosis. *BCL2L12* knockdown experiments support this finding. The reduced viability of mutant lines after *BCL2L12* knockdown and UVR exposure suggests that these lines are dependent on *BCL2L12* expression for survival, a common occurrence known as oncogene addiction (25). In fact, for several of the mutant lines, stable knockdown of *BCL2L12* led to cell death without any exposure to UVR, further supporting the role of BCL2L12 in tumor survival.

Interplay between altered miRNA binding and synonymous mutations has been shown previously. A synonymous mutation in the immunity-related GTPase family M gene altered miR-196 binding and deregulated immunity-related GTPase family M-dependent xenophagy in Crohn disease, implicating a synonymous mutation as a likely causal variant for this disease (26). However, a direct link between a synonymous mutation and the origin of cancer has not been shown. This study, thus, shows that synonymous mutations may be selected in cancer and play a role in tumorigenesis. Importantly, the selection mechanism may possibly be through the relaxation of purifying selection and/or the plasticity–relaxation–mutation mechanism as well as some other alternatives (16, 27–31) rather than positive selection. The data presented here cannot unambiguously select one specific mechanism. However, the presented genetic and functional data support our view that synonymous mutations should receive

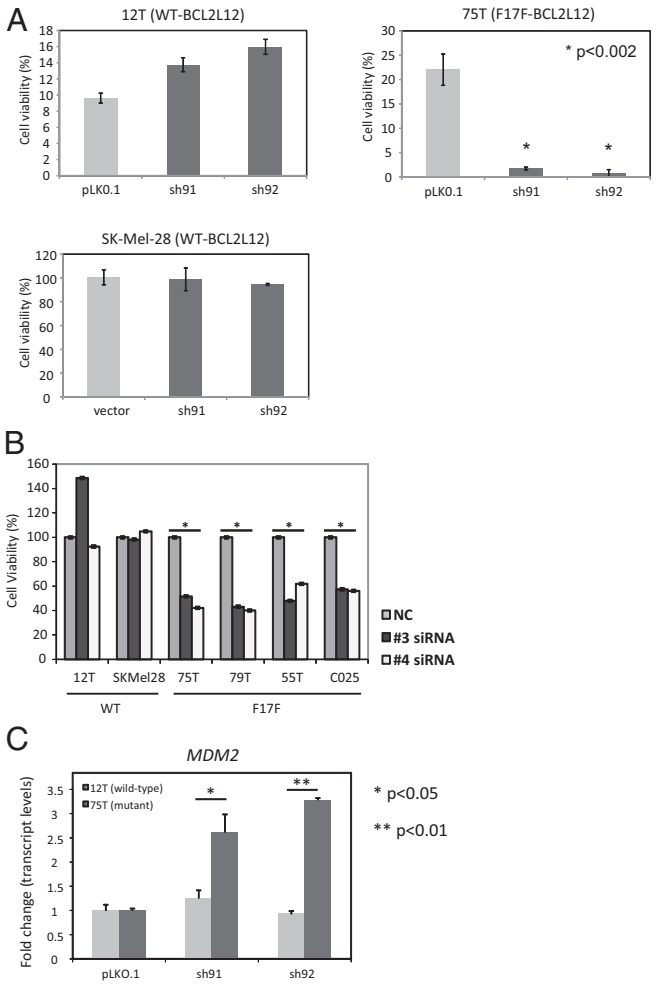

Fig. 3. Effects of the *BCL2L12* (C51T; F17F) recurrent mutation on BCL2L12 function. (*A*) Graphical representation showing the antiapoptotic effect of BCL2L12 mutant cells compared with WT BCL2L12 cells post-UV treatment. The relative cell numbers after the cells were treated for 48 h with UV as estimated by CellTiter-Glo and plotted as percent survival. Error bars are SD. (*B*) Melanoma cells (WT, 12T or SK-Mel-28; mutant, 75T, 79T, 55T, or C025) transiently transfected with *BCL2L12*-specific siRNA were tested for sensitivity to UV-induced cell death. Shown are representative graphs from all cell lines exposed to 50 kμJ UV light. Results were analyzed using Microsoft Excel and GraphPad Prism v5, and graphs are representative of experimental replicates. Error bars are SD (*$P < 0.04$ comparing siRNA with NC). (*C*) qRT-PCR analysis shows that depletion of mutant forms of *BCL2L12* using specific shRNA increases p53-dependent target gene expression compared with depletion of WT *BCL2L12*. Graphs show qRT-PCR analysis of WT *BCL2L12* (12T) and mutant *BCL2L12* (75T) pooled clone mRNA expression levels for *Mdm2*. Results shown are experimental replicates analyzed using Student unpaired *t* test. Error bars are SD. * $P < 0.05$; **$P < 0.01$.

increasing attention, not only in their detection but also in their functional assessment and elucidation of their role in cancer.

Materials and Methods

Tumor Tissues. All DNA samples used in this study were derived from metastases. Samples used for whole-exome capture and prevalence screen were extracted from cell lines established directly from patients' tumors as described previously (32). DNA subjected to whole-genome sequencing was extracted from optimum cutting temperature compound-embedded specimens as described previously (32). The clinical information associated with the melanoma tumors used in this study is provided in *SI Appendix*, Table S2.

DNA Extraction. DNA was extracted using the DNeasy Blood and Tissue Kit (Qiagen) following the manufacturer's instructions. DNA was eluted in 35 μL elution buffer. DNA measurements were made using an ND-1000 UV-Vis spectrophotometer from NanoDrop Technologies.

Whole-Genome Single Nucleotide Variants. For variant calling, only reads with mapping quality of Q30 or greater and bases with quality of Q20 or greater were considered. We used two related algorithms to make single position genotype calls in the normal and melanoma genomes. For all genomes, we used a Bayesian genotype caller named Most Probable Genotype (MPG) that has been described previously (33).

To identify variant positions, we developed an algorithm similar to MPG called Most Probable Variant (MPV). An important distinction between MPG and MPV is that MPV identifies variant positions relative to a reference genotype, whereas MPG identifies genotypes without an a priori reference assumption.

Statistical Calculation of Significance. To evaluate whether the frequency of a synonymous mutation is significantly higher than would be expected if the mutation were neutral, we performed a statistical test. We only considered the validation samples to avoid biases. The null hypothesis is that the probability of a mutation at a specific base is the neutral rate of 11.4 mutations/Mb (i.e., $P = 11.4e\text{-}6$). We computed a one-sided *P* value using the pbinom function in the R statistical software.

Allelic Expression Analyses of Melanoma Samples. Allelic mRNA/cDNA representation analyses shown in Fig. 1*A* were determined using iPlex Gold SBE (Sequenom) using the mel_1 amplification and the mel_X extension primer sets. For each melanoma sample, 12.5 ng cDNA or 20 ng gDNA were aliquotted in 384-well format. Allelic cDNA representation was compared with paired gDNA representation for each sample to identify statistically significant differences. Because cDNA variance did not appear to exhibit a normal distribution, the more conservative Wilcoxon rank sum statistical test was used to determine statistical significance.

Immunoprecipitation and Western Blotting. BCL2L12 subcellular fractionation was performed as previously described (34). Briefly, the BCL2L12 overexpressed HEK293T cells were harvested, washed with ice-cold PBS, and lysed in a hypotonic lysis buffer [10 mM Tris, pH 7.4, 10 mM NaCl, 3 mM $MgCl_2$, 1 mM EDTA, 1 mM EGTA, a mixture protease inhibitors (78415; Thermo Scientific)]. The cells were resuspended in 200 μL lysis buffer, incubated on ice for 10 min, titurated through a p2 tip 15–20 times, and sonicated 2–3 times; the total fraction was centrifuged for 15 min at 375 × *g* at 4 °C, resulting in a pellet that is the nuclear fraction and a supernatant that is the postnuclear fraction. Postnuclear fractions were loaded on 10% (vol/vol) Bris·Tris gel and further analyzed using mouse monoclonal BCL2L12 (1:1,000 dilution; Abcam) fragment antibody. The same membrane also processed later with GAPDH antibody.

HEK293 cells transiently transfected with *BCL2L12*-FLAG (WT, mutant, or empty vector) were gently washed two times in PBS and then lysed using 1.0 mL 1% Nonidet P-40 lysis buffer [1% Nonidet P-40, 50 mM Tris·HCl, pH 7.5, 150 mM NaCl, Complete Protease Inhibitor tablet, EDTA-free (Roche), 1 μM sodium orthovanadate, 1 mM sodium fluoride, 0.1% β-mercaptoethanol] per T-75 flask for 20 min on ice. Lysed cells were scraped and transferred into a 1.5-mL microcentrifuge tube. Extracts were centrifuged for 10 min at 20,000 × *g* at 4 °C; 800 μL supernatant were immunoprecipitated overnight using 30 μL anti-FLAG (M2) beads (Sigma Aldrich). The immunoprecipitates were washed and subjected to SDS/PAGE and Western blotting as previously described (32).

Lentiviral shRNA. Constructs for stable depletion of *BCL2L12* (RHS45330-NM_138639) were obtained from Open Biosystems and confirmed to efficiently knockdown BCL2L12 at the protein level. Lentiviral stocks were prepared as previously described (35). Melanoma cell lines were infected with shRNA lentiviruses for each condition (vector and two different *BCL2L12*-specific shRNAs). Selection of stable pooled clones was done in the presence of 3 μg/mL puromycin containing normal medium for 3–5 d before determining knockdown efficiency.

siRNA Depletion of Endogenous *BCL2L12* in Melanoma Cells. Specific siRNA was purchased from Dharmacon (Thermo Fisher Scientific) designed using their siRNA design program for human *BCL2L12*. Four independent siRNA molecules were used to transiently deplete *BCL2L12* in malignant melanoma cells. Using DharmaEffect transfection reagent #1 specific for siRNA, melanoma cells were tranfected with 50 nM siRNA molecules (#3 and #4) in the presence of OptiMEM-I medium after cells were seeded into 96-well plates at a density of 2,000 cells/well 24 h before transfection. Cells were incubated for 24 h posttransfection before application of any genotoxic stressors.

Cell Viability Assays. Stably depleted pooled clones were seeded into 96-well clear bottom opaque plates at 1,000 cells per well. Cells were incubated 24 h before exposure to UV light (50 kμJ) using a UV Stratalinker 2400 (Stratagene). Plates were then incubated for an additional 48 h before testing for cell viability using Cell-Titer-Glo (G7571). Plates were analyzed on a Thermo Electron Luminoskan reader. Data were then analyzed using Microsoft Excel to generate graphs and statistics.

miRNA Target Site Prediction. We used the two miRNA target site prediction platforms PITA (19) and miRanda (20) to search for miRNA target site predictions that overlap the C51T mutated position in *BCL2L12*. We executed them with default prediction parameters and found that both platforms predict hsa-miR-671–5p to target the WT *BCL2L12* mRNA overlapping position 51 but not the mutant mRNA.

miRNA Depletion of Endogenous *BCL2L12* in Melanoma Cells A. Specific miRNA mimetic (hsa-miR-671–5p) was purchased from Sigma Aldrich (HMI0901) that was determined to potentially target human *BCL2L12*. A negative control scrambled miR (NC) was purchased from Dharmacon (CN-001000-01; Thermo Fisher Scientific). Using DharmaFECT transfection reagent #1 (T-2001) specific for siRNA or miRNA, melanoma cells were tranfected with 20 nM has-miR-671–5p or NC molecules in the presence of OptiMEM-I medium after cells were seeded into six-well plates at a density of 200,000 cells/well 24 h before transfection. Cells were incubated for 24 h posttransfection before extraction of miRNA and mRNA and qRT-PCR analysis.

Anti–miR-671–5p Rescue Assay. A specific anti-miRNA mimic (anti–hsa-miR-671–5p) was purchased from Qiagen (MIN0003880), which was determined to inhibit the hsa-miR-671–5p mimic. An NC was purchased from Dharmacon (Thermo Fisher Scientific). Using DharmaEffect transfection reagent #1 specific for siRNA or miRNA, melanoma cells were cotranfected with 20 nM hsa-miR-671–5p or NC molecules plus either 0 or 50 nM anti–miR-671–5p in the presence of OptiMEM-I medium after cells were seeded into six-well plates at a density of 200,000 cells/well 24 h before transfection. Cells were incubated for 24 h posttransfection before extraction of miRNA and mRNA and qRT-PCR analysis.

Real-Time qPCR of miRNA Targeted Cell Lines. miRNA and mRNA were extracted from transiently transfected melanoma to assess for knockdown of endogenous *BCL2L12* following the manufacturer's protocol for the miRNeasy Mini Kit (217004; QIAGEN); 1 μg total RNA was used for cDNA synthesis using an miScript II Reverse Transcription Kit (218193; QIAGEN). cDNA was amplified with the 5× HiFlex buffer to quantitate in parallel the miRNA and mRNA. To test for loss of *BCL2L12* message, we followed the manufacturer's protocol and mixed primers and cDNA with QuantiTect SYBR Green PCR master mix at a final volume of 10 μL in triplicate (QIAGEN). qRT-PCR analysis was done using the ABI 7900HT Fast Real-Time PCR System. Results were analyzed using Microsoft Excel and GraphPad Prism v5.0.

miRNA Rescue Experiment. A modified form of the hsa-miR-671–5p was custom made from Sigma Aldrich, with a single site changed to represent the synonymous mutation found in melanoma. Melanoma cells were seeded at ∼300,000 cells per well in six-well plates and incubated overnight before transient transfection. Cells were transfected with hsa-miR-671–5p (miR), mod-hsa-miR-671–5p (mod-miR), or NC in triplicate; total miRNA/RNA was amplified using the miScript miRNA cDNA Kit from Qiagen, and levels of BCL2L12 message were detected using SYBR Green master mix (Qiagen) in triplicate. GAPDH was used as an internal control to normalize between samples and generate graphs using Microsoft Excel. All experiments were repeated two to three times.

ACKNOWLEDGMENTS. We thank Drs. Chris Schmidt and Peter Parsons for establishment of the majority of melanoma cell lines and V. Maduro, H. Ozel Abaan, and P. Cruz for generating the sequence data analyzed here. We thank Dr. V. G. Prieto for pathologic review of the biospecimens from the Melanoma Informatics, Tissue Resource, and Pathology Core (MelCore) at MD Anderson. We thank Dr. T. Wolfsberg for bioinformatics help, J. Jiang for sequencing help, and J. Fekecs and D. Leja for graphical assistance. We thank Drs. T. Barber and M. Willard for critical comments on the manuscript. S.C.J.P. is supported by an NIGMS Postdoctoral Research Associate (PRAT) Fellowship. This work was supported by the Intramural Research Programs of the National Human Genome Research Institute, by the Henry Chanoch Krenter Institute for Biomedical Imaging and Genomics, the estate of Alice Schwarz-Gardos, the estate of John Hunter, the Knell Family, the Peter and Patricia Gruber Award, National Cancer Institute Grant R21CA152432 (to R.K.), the National Institutes of Health, University of Texas MD Anderson Cancer Center Melanoma Specialized Programs of Research Excellence Grant P50 CA093459, Cancer Center Support Grant (CCSG) Core Grant NCI 5P30 CA006516-46 (to G.P.), the Human Frontier Science Program RGP0024 Grant (to A.A.K.), National Health and Medical Research Council of Australia Grants 1026112 and 613686, and a public–private partnership between the Intramural Research Programs of the National Human Genome Research Institute, the National Cancer Institute, and Eli Lilly and Company coordinated by the Foundation for the National Institutes of Health.

1. Wei X, et al. (2011) Exome sequencing identifies GRIN2A as frequently mutated in melanoma. *Nat Genet* 43(5):442–446.
2. Hodis E, et al. (2012) A landscape of driver mutations in melanoma. *Cell* 150(2):251–263.
3. Berger MF, et al. (2012) Melanoma genome sequencing reveals frequent PREX2 mutations. *Nature* 485(7399):502–506.
4. Krauthammer M, et al. (2012) Exome sequencing identifies recurrent somatic RAC1 mutations in melanoma. *Nat Genet* 44(9):1006–1014.
5. Nikolaev SI, et al. (2012) Exome sequencing identifies recurrent somatic MAP2K1 and MAP2K2 mutations in melanoma. *Nat Genet* 44(2):133–139.
6. Stark MS, et al. (2012) Frequent somatic mutations in MAP3K5 and MAP3K9 in metastatic melanoma identified by exome sequencing. *Nat Genet* 44(2):165–169.
7. Huang FW, et al. (2013) Highly recurrent TERT promoter mutations in human melanoma. *Science* 339(6122):957–959.
8. Horn S, et al. (2013) TERT promoter mutations in familial and sporadic melanoma. *Science* 339(6122):959–961.
9. Parker SC, et al. (2012) Mutational signatures of de-differentiation in functional non-coding regions of melanoma genomes. *PLoS Genet* 8(8):e1002871.
10. Pleasance ED, et al. (2010) A comprehensive catalogue of somatic mutations from a human cancer genome. *Nature* 463(7278):191–196.
11. Sjoblom T, et al. (2006) The consensus coding sequences of human breast and colorectal cancers. *Science* 314(5797):268–274.
12. Greenman C, et al. (2007) Patterns of somatic mutation in human cancer genomes. *Nature* 446(7132):153–158.
13. Davies H, et al. (2002) Mutations of the BRAF gene in human cancer. *Nature* 417 (6892):949–954.
14. Kimchi-Sarfaty C, et al. (2007) A "silent" polymorphism in the MDR1 gene changes substrate specificity. *Science* 315(5811):525–528.
15. Chamary JV, Parmley JL, Hurst LD (2006) Hearing silence: Non-neutral evolution at synonymous sites in mammals. *Nat Rev Genet* 7(2):98–108.
16. Hughes AL (2012) Evolution of adaptive phenotypic traits without positive Darwinian selection. *Heredity (Edinb)* 108(4):347–353.
17. Stegh AH, et al. (2010) Glioma oncoprotein Bcl2L12 inhibits the p53 tumor suppressor. *Genes Dev* 24(19):2194–2204.
18. Sauna ZE, Kimchi-Sarfaty C (2011) Understanding the contribution of synonymous mutations to human disease. *Nat Rev Genet* 12(10):683–691.
19. Kertesz M, Iovino N, Unnerstall U, Gaul U, Segal E (2007) The role of site accessibility in microRNA target recognition. *Nat Genet* 39(10):1278–1284.
20. John B, et al. (2004) Human microRNA targets. *PLoS Biol* 2(11):e363.
21. Cooper GM, et al. (2005) Distribution and intensity of constraint in mammalian genomic sequence. *Genome Res* 15(7):901–913.
22. Davydov EV, et al. (2010) Identifying a high fraction of the human genome to be under selective constraint using GERP++. *PLoS Comput Biol* 6(12):e1001025.
23. Goode DL, et al. (2010) Evolutionary constraint facilitates interpretation of genetic variation in resequenced human genomes. *Genome Res* 20(3):301–310.
24. Stark MS, et al. (2010) Characterization of the melanoma miRNAome by deep sequencing. *PLoS One* 5(3):e9685.
25. Weinstein IB, Joe AK (2006) Mechanisms of disease: Oncogene addiction—a rationale for molecular targeting in cancer therapy. *Nat Clin Pract Oncol* 3(8):448–457.
26. Brest P, et al. (2011) A synonymous variant in IRGM alters a binding site for miR-196 and causes deregulation of IRGM-dependent xenophagy in Crohn's disease. *Nat Genet* 43(3):242–245.
27. Hughes AL (2007) Looking for Darwin in all the wrong places: The misguided quest for positive selection at the nucleotide sequence level. *Heredity (Edinb)* 99(4):364–373.
28. Hughes AL (2008) The origin of adaptive phenotypes. *Proc Natl Acad Sci USA* 105(36): 13193–13194.
29. Nei M (2005) Selectionism and neutralism in molecular evolution. *Mol Biol Evol* 22(12): 2318–2342.
30. Jensen JD, Thornton KR, Bustamante CD, Aquadro CF (2007) On the utility of linkage disequilibrium as a statistic for identifying targets of positive selection in non-equilibrium populations. *Genetics* 176(4):2371–2379.
31. Nishi N, Odagaki Y, Koyama T (2000) Pharmacological characterization of metabotropic glutamate receptor-mediated high-affinity GTPase activity in rat cerebral cortical membranes. *Br J Pharmacol* 130(7):1664–1670.
32. Palavalli LH, et al. (2009) Analysis of the matrix metalloproteinase family reveals that MMP8 is often mutated in melanoma. *Nat Genet* 41(5):518–520.
33. Teer JK, et al. (2010) Systematic comparison of three genomic enrichment methods for massively parallel DNA sequencing. *Genome Res* 20(10):1420–1431.
34. Fazioli F, et al. (1993) Eps8, a substrate for the epidermal growth factor receptor kinase, enhances EGF-dependent mitogenic signals. *EMBO J* 12(10):3799–3808.
35. Prickett TD, et al. (2009) Analysis of the tyrosine kinome in melanoma reveals recurrent mutations in ERBB4. *Nat Genet* 41(10):1127–1132.